Regenerative Medicine and Dentistry
https://www.sciltp.com/journals/rmd

Supplementary Materials

Single-Cell Re-Mining Identifies a Pathogenic Fibroblast Subpopulation and Nominates Exploratory Therapeutic Hypotheses in Human Bone Nonunion

Hang Chen [1,2], Chang Lei [2,3], Xiao Liu [4], Xiaobo Chen [5], Shufang Luo [5] and Chun Xu [1,2,6,*]

[1] Sydney Dental School, Faculty of Medicine and Health, The University of Sydney, Sydney, NSW 2006, Australia
[2] Charles Perkins Centre, The University of Sydney, Camperdown, NSW 2006, Australia
[3] School of Medical Science, Faculty of Medicine and Health, The University of Sydney, Sydney, NSW 2006, Australia
[4] Intelligent Polymer Research Institute, Innovation Campus, University of Wollongong, Wollongong, NSW 2522, Australia
[5] Stomatological Hospital of Xiamen Medical College, Xiamen Key Laboratory of Stomatological Disease Diagnosis and Treatment, Xiamen 361000, China
[6] Sydney Nano Institute, The University of Sydney, Sydney, NSW 2006, Australia
* Correspondence: chun.xu@sydney.edu.au

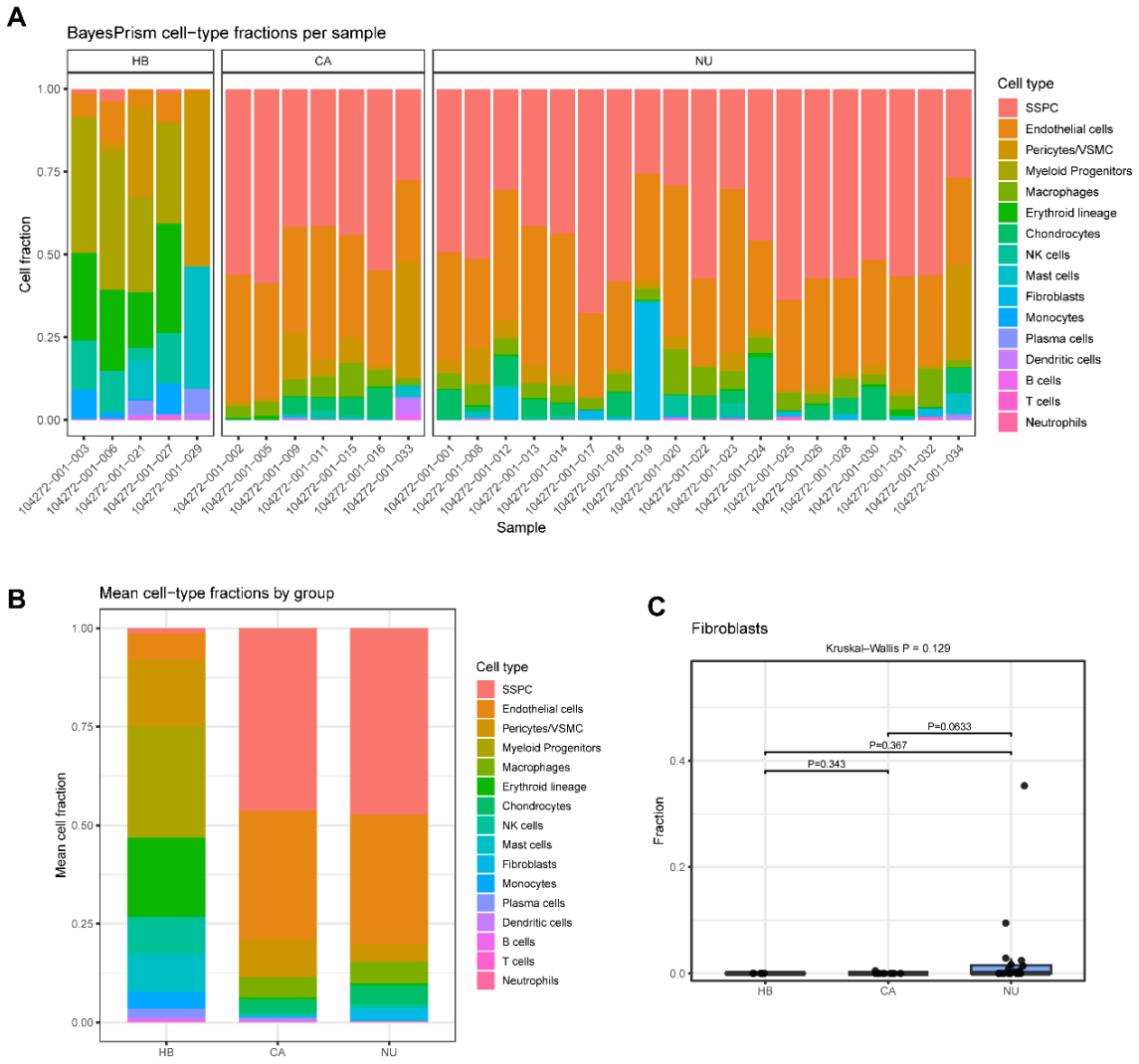

Figure S1. External comparison with the published GSE226568/GSE226566 bulk RNA-seq cohort using reference-guided deconvolution. (**A**) Sample-level inferred cell-type fractions for the external bulk RNA-seq cohort. (**B**) Group-averaged inferred cell-type composition across healthy bone (HB), fracture callus (CA), and nonunion (NU) samples. (**C**) Sample-level inferred fibroblast fractions across groups. Points indicate individual samples. *p* values shown correspond to the Kruskal–Wallis test and pairwise Wilcoxon rank-sum tests.

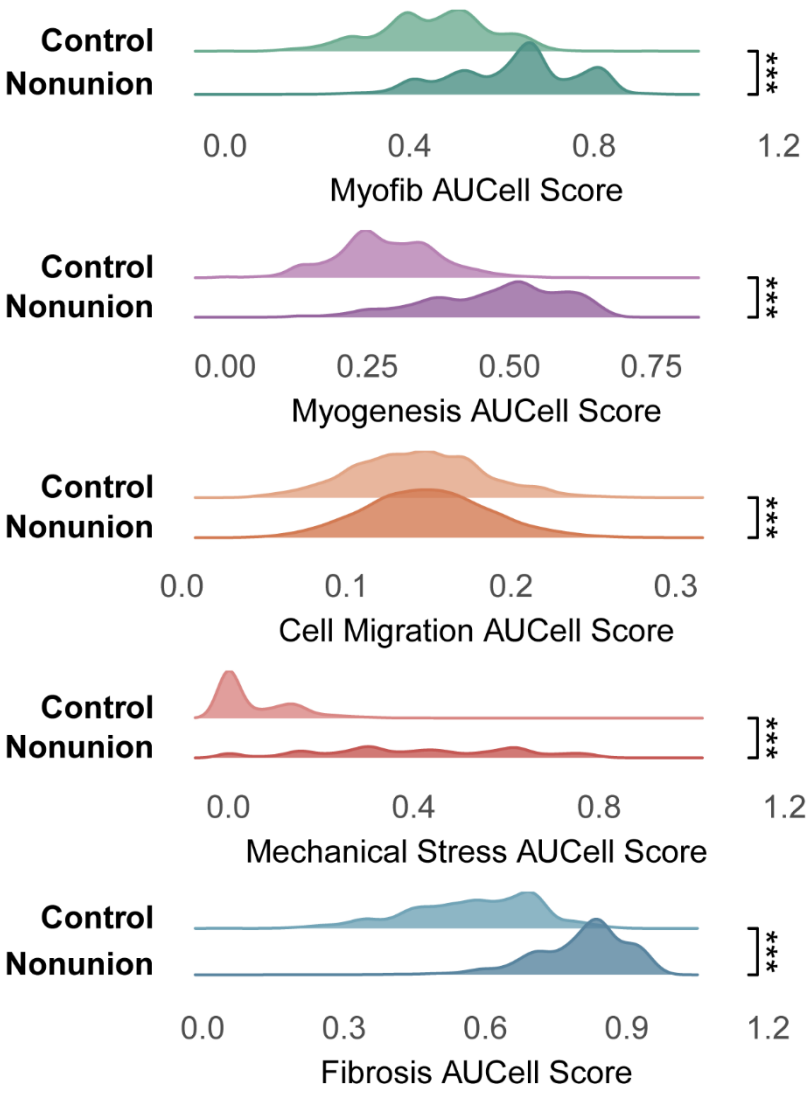

Figure S2. Ridge plots comparing functional pathway scores (Migration, Mechanical, Fibrosis, Myofib, and Myogenesis) between control and Nonunion fibroblasts using "AUCell".

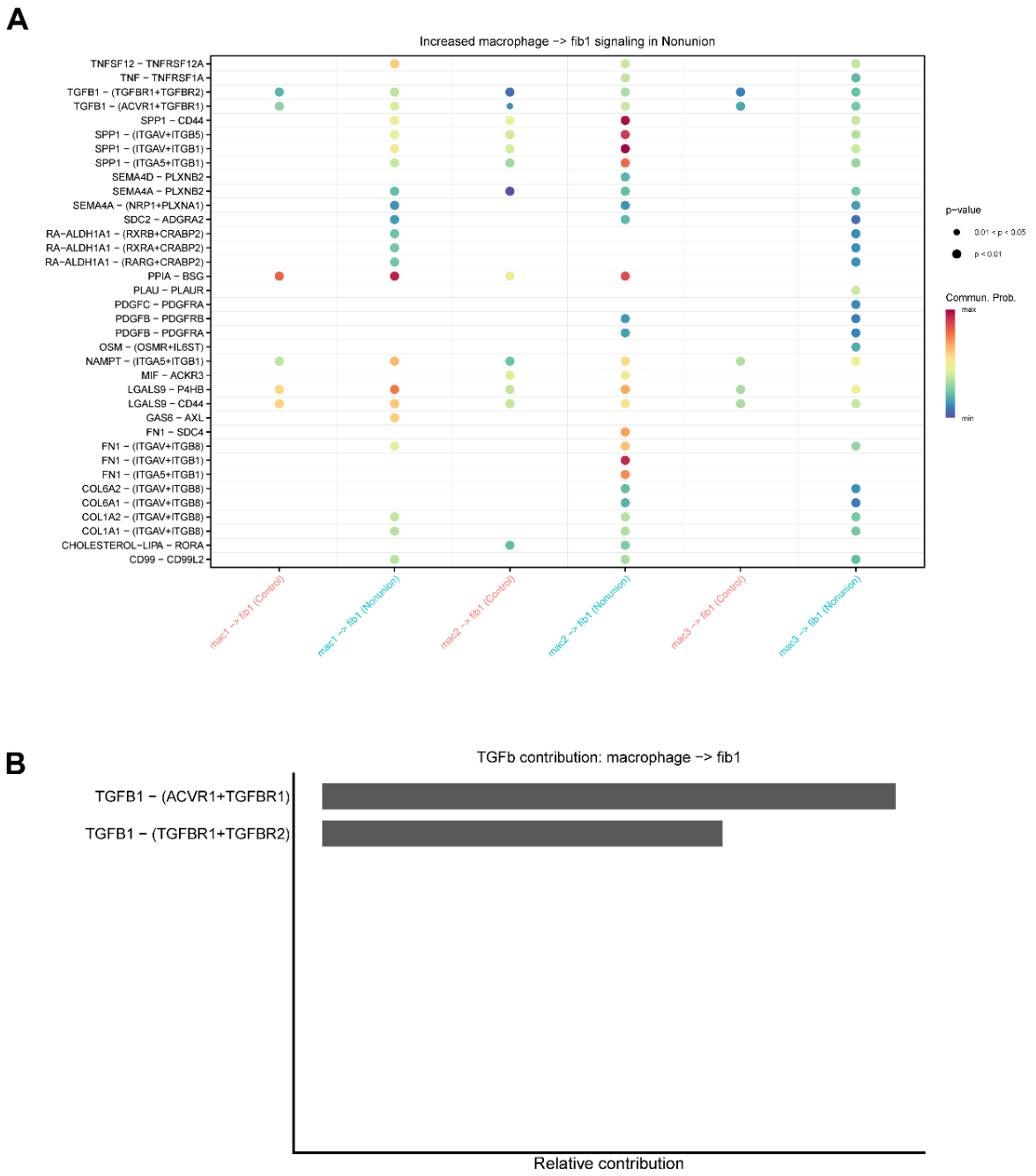

Figure S3. Subtype-resolved macrophage-to-Fib1 communication in nonunion. (**A**) Bubble plot showing ligand–receptor interactions increased in nonunion for macrophage-subtype-to-Fib1 communication, directly extracted from the subtype-resolved CellChat analysis after fibroblast/macrophage subclustering. (**B**) Contribution analysis of the TGF-β pathway in nonunion, highlighting TGF-β as a representative signaling route within the macrophage-to-Fib1 axis.

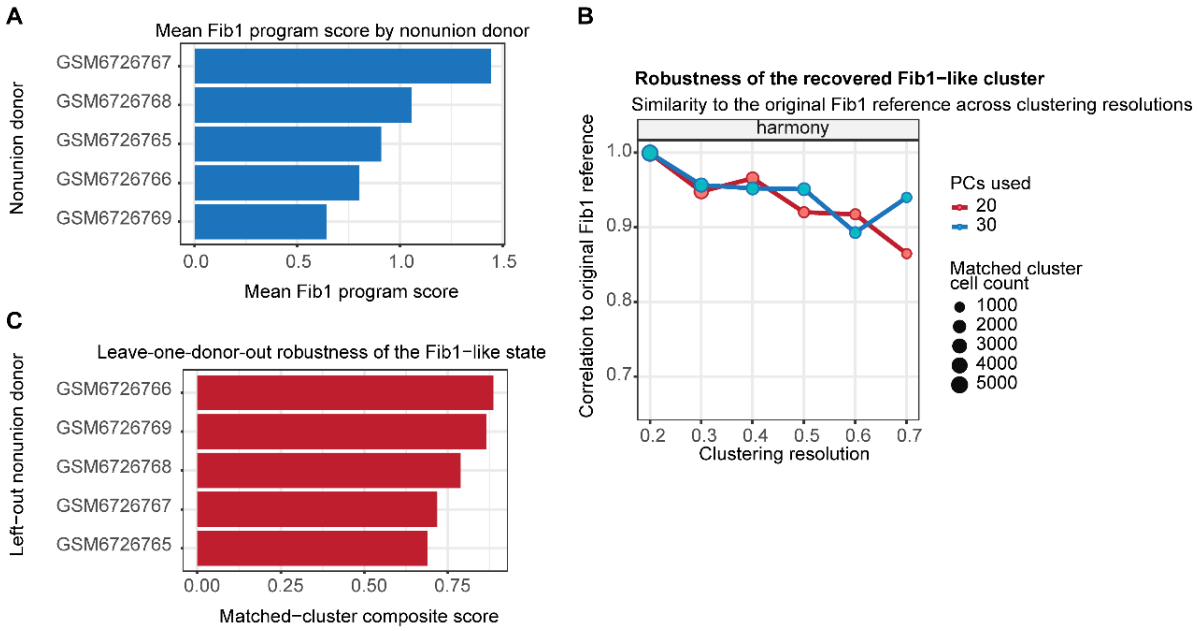

Figure S4. Reproducibility and robustness of the Fib1-like fibroblast state in nonunion. (**A**) Donor-level summary of Fib1 program activity across nonunion donors, shown as mean Fib1 program score for each donor. (**B**) Robustness of the recovered Fib1-like cluster across alternative clustering resolutions and dimensional settings, shown as similarity to the original Fib1 reference program; point size indicates the size of the matched cluster. (**C**) Leave-one-donor-out analysis showing that a Fib1-like state remained recoverable after sequential exclusion of each nonunion donor, summarized by matched-cluster composite score.

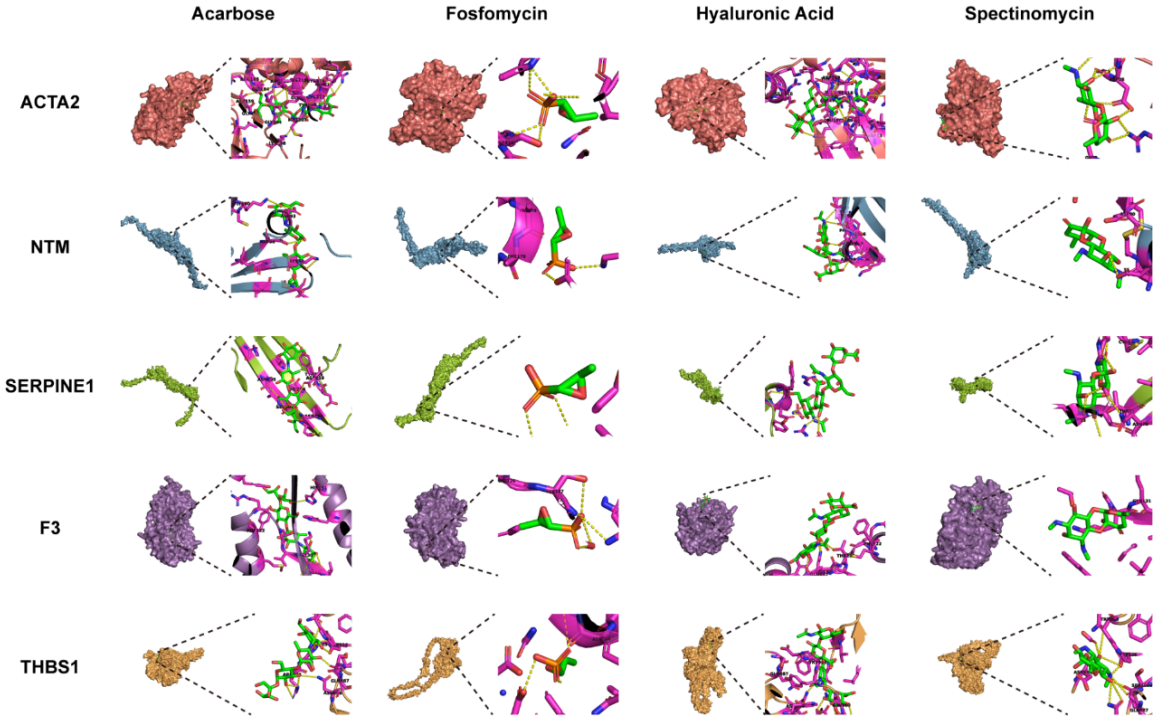

Figure S5. Predicted binding mode of Fib1 target proteins with potential candidate drugs generated by Boltz2.